

Characterization of *Shewanella oneidensis* MtrC: a cell-surface decaheme cytochrome involved in respiratory electron transport to extracellular electron acceptors

Robert S. Hartshorne · Brian N. Jepson · Tom A. Clarke · Sarah J. Field · Jim Fredrickson · John Zachara · Liang Shi · Julea N. Butt · David J. Richardson

Received: 18 April 2007 / Accepted: 9 July 2007 / Published online: 14 August 2007
© SBIC 2007

Abstract MtrC is a decaheme *c*-type cytochrome associated with the outer cell membrane of Fe(III)-respiring species of the *Shewanella* genus. It is proposed to play a role in anaerobic respiration by mediating electron transfer to extracellular mineral oxides that can serve as terminal electron acceptors. The present work presents the first spectropotentiometric and voltammetric characterization of MtrC, using protein purified from *Shewanella oneidensis* MR-1. Potentiometric titrations, monitored by UV–vis absorption and electron paramagnetic resonance (EPR) spectroscopy, reveal that the hemes within MtrC titrate over a broad potential range spanning between approximately +100 and approximately –500 mV (vs. the standard hydrogen electrode). Across this potential window the UV–vis absorption spectra are characteristic of low-spin *c*-type hemes and the EPR spectra reveal broad, complex features that suggest the presence of magnetically spin-coupled low-spin *c*-hemes. Non-catalytic protein film voltammetry of MtrC demonstrates reversible electrochemistry over a potential window similar to that disclosed spectroscopically. The voltammetry also allows definition of kinetic properties

of MtrC in direct electron exchange with a solid electrode surface and during reduction of a model Fe(III) substrate. Taken together, the data provide quantitative information on the potential domain in which MtrC can operate.

Keywords Cytochrome *c* · Iron respiration · Electron transfer · Protein film voltammetry · Electron paramagnetic resonance

Abbreviations

CAPS	3-(Cyclohexyl)-1-aminopropanesulfonic acid
CHAPS	3-[(3-Cholamidopropyl)dimethylammonio]propanesulfonic acid
CHES	<i>N</i> -Cyclohexyl-2-aminoethanesulfonic acid
EPR	Electron paramagnetic resonance
HEPES	<i>N</i> -(2-Hydroxyethyl)piperazine- <i>N'</i> -ethanesulfonic acid
MES	2-Morpholinoethanesulfonic acid
MQH ₂	Menaquinol
PAGE	Polyacrylamide gel electrophoresis
PFV	Protein film voltammetry
SDS	Sodium dodecyl sulfate
SHE	Standard hydrogen electrode

R. S. Hartshorne · B. N. Jepson · T. A. Clarke · S. J. Field · J. N. Butt (✉) · D. J. Richardson (✉)
Centre for Metalloprotein Spectroscopy and Biology,
School of Biological Sciences and School of Chemical
Sciences and Pharmacy,
University of East Anglia,
Norwich NR4 7TJ, UK
e-mail: j.butt@uea.ac.uk

D. J. Richardson
e-mail: d.richardson@uea.ac.uk

J. Fredrickson · J. Zachara · L. Shi
Pacific Northwest National Laboratory,
P.O. Box 999, Richland,
WA 99352, USA

Introduction

Members of the *Shewanella* species are Gram-negative γ -proteobacteria and have been isolated from many aquatic and marine environments [1]. *Shewanella* species are renowned for their incredible respiratory versatility and are reportedly able to use over 20 terminal electron acceptors for respiration [2, 3]. These include metal oxide minerals, particularly those of Fe(III), such as hematite and goethite.

Fe(III) mineral oxide reduction is one of the most widespread respiratory processes in anoxic zones and has environmental significance, influencing several biogeochemical cycles [4–7]. Fe(III) is highly insoluble in most environments at circumneutral pH and, unlike other terminal electron acceptors such as oxygen, nitrate and sulfate, cannot freely diffuse into cells. For respiration of insoluble substrates the bacterium must transfer electrons from the central cell metabolism to the iron(III) oxide surface. It is generally considered that electrons are transferred by electron transfer proteins (or quinones), in the inner membrane, to a series of multiheme *c*-type cytochromes. These cytochromes transfer electrons from the periplasm to the extracellular side of the outer cell membrane and across the microbe–mineral oxidant interface [5, 8–11].

Electron transport proteins proposed to be involved in Fe(III) respiration in *Shewanella oneidensis* MR-1 include an inner-membrane periplasmic tetraheme quinol dehydrogenase (CymA) [8, 12], two periplasmic decaheme cytochromes (MtrD and MtrA) [10, 13], periplasmic tetraheme cytochrome (Stc) [14, 15], the cytochrome domain of Fe(III)-induced flavocytochrome c_3 , [16] two putative outer-membrane β -barrel proteins (MtrE and MtrB) [17–19] and three outer-membrane decaheme cytochromes (MtrF, OmcA and MtrC) [11, 18, 20, 21]. Although genetic studies have identified specific proteins that are involved in Fe(III) respiration in *Shewanella* sp. [8–11, 13, 14, 17], mechanistic details of the electron transfer process are as yet unknown. It is postulated that following oxidation of menaquinol (MQH₂) by CymA, electrons are transferred via periplasmic multiheme cytochromes (MtrA and/or Stc)

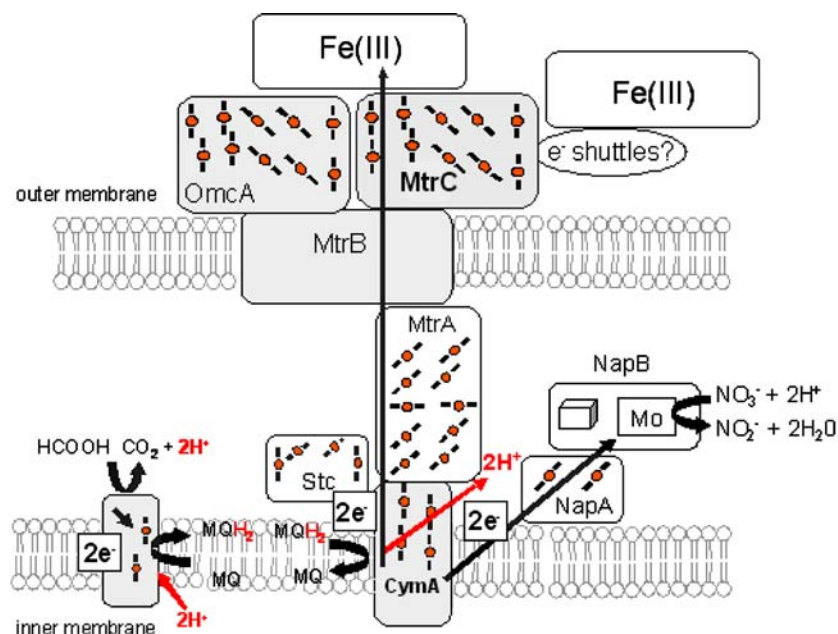
to outer-membrane-associated multiheme cytochromes, OmcA and MtrC (Fig. 1) [5, 8–11, 13, 14, 16–18]. OmcA and MtrC protein sequences both comprise ten putative *c*-heme binding site motifs (CXXCH, where X is any residue) and a lipid-binding motif for anchoring to the outer membrane [11, 22]. Because of their proposed location, these multiheme cytochromes are believed to function in Fe(III) respiration by mediating electron transfer across the microbe–mineral oxidant interface [5, 10, 13, 18, 22]. Significantly, a $\Delta mtrC$ strain of *S. oneidensis* MR-1 displayed a marked decrease in the ability to respire iron(III) oxides and iron(III) citrate, while retaining the ability to respire soluble terminal electron acceptors, including NO₃⁻ and NO₂⁻ [11, 17]. In the light of this, we present here the first spectroscopic characterization of the decaheme cytochrome MtrC. Data obtained from potentiometric and voltammetric analysis provide quantitative information on the potential and time domains in which MtrC can operate that can be considered alongside whole-cell electrochemical studies on *Shewanella* species and their use in microbial fuel cells [23, 24].

Materials and methods

Growth conditions and protein purification

Cultures of the *S. oneidensis* MR-1 expression strain LS306, encoding MtrC with a C-terminus tag [21, 25], were grown aerobically in Luria–Bertani medium (containing 50 $\mu\text{g mL}^{-1}$ kanamycin) at 303 K overnight. For scale-up, each initial overnight culture (10 mL) was used to

Fig. 1 An electron transfer scheme for Fe(III) mineral oxides and nitrate reduction in *Shewanella oneidensis*



inoculate 1 L of fresh Luria–Bertani medium (containing $50 \mu\text{g mL}^{-1}$ kanamycin). For standard MtrC preparations, ten such 1 L cultures were grown aerobically at 303 K until an optical density at 600 nm of 0.6 was achieved and were then induced with 1 mM L-arabinose. Cells were harvested by centrifugation (6,000g, 277 K, 15 min), washed, and resuspended in 20 mM *N*-(2-hydroxyethyl)piperazine-*N'*-ethanesulfonic acid (HEPES), pH 7.6. Cell lysis was achieved by three passes through a French pressure cell operated at 1,000 psi. Unbroken cells and cell debris were removed by centrifugation (15,000g, 277 K, 1 h). The supernatant was centrifuged (150,000g, 277 K, 1 h) and the resulting pellet (i.e., the dark-red membrane fraction) was solubilized in 20 mM HEPES, pH 7.6, 0.5% (wt/vol) 3-[(3-cholamidopropyl)dimethylammonio]propanesulfonic acid (CHAPS) (Buffer A), with gentle stirring for 4 h at 277 K. Unsolubilized proteins were removed by centrifugation at 15,000g and 277 K for 30 min. The solubilized membrane fraction was applied to a (diethylamino)ethyl-Sepharose CL-6B anion-exchange column (Amersham Pharmacia Biotech) preequilibrated with buffer A. The column was washed with buffer A (four column volumes) and developed with a NaCl gradient (0–1 M). The eluted fractions containing MtrC were identified by a combination of sodium dodecyl sulfate (SDS) polyacrylamide gel electrophoresis (PAGE) and heme-linked peroxidase staining. MtrC was eluted at approximately 250 mM NaCl. Fractions containing MtrC were combined, dialyzed against 20 mM HEPES, pH 7.6, 0.5% (wt/vol) CHAPS, 100 mM NaCl (buffer B) and concentrated by ultrafiltration (30-kDa cutoff membrane, Amicon). The sample was applied to an S200 HR 10/30 column (Amersham Biosciences) preequilibrated with buffer B. The column was developed with equilibration buffer and fractions containing MtrC were combined and then applied to an Econo-Pack High-Q cartridge (Bio-Rad, Hercules, CA, USA) preequilibrated with buffer B. The column was washed with equilibration buffer (five column volumes) and developed with a NaCl gradient (0.1–1 M). MtrC was eluted at approximately 0.45 M NaCl. Fractions containing MtrC were dialyzed against 20 mM HEPES, pH 7.5, 100 mM NaCl, 0.5% (wt/vol) CHAPS and concentrated by ultrafiltration (30-kDa cutoff membrane, Amicon). Aliquots of purified MtrC were frozen in liquid nitrogen and stored at 193 K. Protein concentration was determined using the Bradford method with bovine serum albumin serving as the standard. The concentration of purified MtrC was also determined by UV–vis absorption spectroscopy of the air-equilibrated protein using the experimentally determined $\epsilon_{410 \text{ nm}} = 1,260 \text{ mM}^{-1} \text{ cm}^{-1}$. For quantification of the number of covalently ligated *c*-type hemes attached to MtrC, conversion into pyridine derivatives was achieved by incubating protein (3 μM) with pyridine

(2.1 M) and NaOH (75 mM) in water at room temperature for 15 min. Sodium dithionite and potassium ferricyanide were then added to separate aliquots of the resulting solution such that the final concentrations of protein, reductant and oxidant were 2.5 μM , 1.5 mM and 750 μM , respectively. Heme content was determined using the difference molar absorption coefficient of $19.1 \text{ mM}^{-1} \text{ cm}^{-1}$ at 550 nm for the pyridine ferroheme minus the pyridine ferriheme [26].

SDS-PAGE and Western blotting

Slab gels of 12% (wt/vol) polyacrylamide were employed for resolution of proteins, with samples being loaded via a stacking gel of 5% (wt/vol) polyacrylamide. Samples were prepared for electrophoresis by incubation with 3 M urea/90 mM SDS at 363 K for 10 min. The presence of *c*-type cytochromes was probed for using a heme-linked peroxidase staining method [27]. Western blotting was performed using a peptide-specific affinity purified anti-MtrC antibody with goat-anti rabbit alkaline phosphatase secondary antibody (Sigma). A 5-bromo-4-chloro-3-indolyl phosphate/nitro blue tetrazolium colorimetric assay (Sigma) was used for signal detection.

UV–vis spectropotentiometric titrations

Spectropotentiometric titrations of a 2 μM MtrC solution in 100 mM HEPES, 100 mM NaCl, 0.5% (wt/vol) CHAPS, pH 7.5 were performed as described previously [28] in the presence of redox mediators. The mediators (10 μM each) were diaminodurene, phenazine methosulfate, phenazine ethosulfate, anthraquinone 2,6-sulfonate, anthraquinone 2-sulfonate, benzyl viologen and methyl viologen. The titrations were performed at 288 K and UV–vis absorption spectra from 500 to 600 nm were collected in situ at a range of potentials in both reductive (using sodium dithionite) and oxidative (using potassium ferricyanide) titers. The change in α -peak absorbance (referenced vs. a 562-nm isosbestic point) was used to monitor the extent of MtrC reduction and a plot of the fraction of reduced MtrC as a function of potential was constructed. Measurements prior to, and following, titrations confirmed that the solution pH did not change during experimentation.

Electron paramagnetic resonance spectroscopy

Low-temperature electron paramagnetic resonance (EPR) spectroscopy was performed at X-band frequency, using an ER200D spectrometer. The microwave bridge and

electromagnet were interfaced to an EMX control (Bruker Biospin, Germany). A dual-mode X-band cavity (Bruker, type ER116DM) was used, where the sample temperature was modulated using an ESR-900 liquid helium flow cryostat. Spin quantification of the EPR signals were estimated by double integration and comparison with a 1 mM Cu^{2+} -EDTA standard, all measured under nonsaturating conditions [29]. Redox poisoning of samples of MtrC (140 μM) in 50 mM HEPES, 100 mM NaCl, 0.5% (wt/vol) CHAPS, pH 7.5 for EPR analysis was achieved under the control of a potentiostat (Autolab electrochemical analyzer under the control of GPES software) using a three-electrode cell configuration housed in an anaerobic chamber (nitrogen atmosphere with less than 2 ppm O_2). Samples were introduced into a freshly polished glassy carbon pot thermostated at 288 K that constituted the working electrode. A platinum wire counter electrode was housed in a chamber separated from the MtrC solution via a Vycor frit and the Ag/AgCl, KCl (saturated) reference electrode (298 K) was in contact with the sample through a Luggin capillary tip. To facilitate electrode–MtrC equilibration a mediator solution comprising diaminodurene, phenazine methosulfate, phenazine ethosulfate, anthraquinone 2,6-sulfonate, anthraquinone 2-sulfonate, benzyl viologen and methyl viologen (all at 20 μM final concentration) was added to the MtrC sample. Samples were poised at the desired potential, with stirring, until the current from the sample fell to zero, indicating equilibration with the applied potential. Equilibration at each potential typically occurred within 30 min. After the zero current potential of the cell had been confirmed to be the desired equilibration potential, a 100- μL sample was immediately transferred with a gastight syringe into a custom-built quartz EPR tube (4-mm internal diameter). The gastight syringe was placed in the glove box at least 3 days before samples were poised to minimize the possibility for oxygen introduction into the sample. The EPR tubes were then rapidly sealed with Parafilm, removed from the glove box and immediately placed in liquid nitrogen, in which the sample froze over a period of 30–45 s. Potentials are reported with reference to the standard hydrogen electrode (SHE) by addition of 197 mV to those measured.

Sedimentation equilibrium analysis

Experiments were performed using a Beckman Optima XL-I analytical ultracentrifuge equipped with scanning absorption optics and an An50Ti rotor. The MtrC partial specific volume of 0.721 mL g^{-1} was estimated from the amino acid sequence using SEDNTERP software [30]. MtrC samples were diluted to appropriate concentrations with 50 mM HEPES, 150 mM NaCl, 0.5% (wt/vol)

CHAPS, pH 7.5 and loaded into charcoal-filled Epon double-sector cells fitted with quartz windows. Reference sectors were filled with 120 μL buffer. Sedimentation equilibrium experiments were performed at 293 K at 6,000, 8,000 and 10,000 rpm. Concentration profiles were measured at absorption wavelengths of 440 nm (3 μM), 530 nm (10 μM), 495 nm (20 μM), 600 nm (40 μM) and 620 nm (60 μM) for the MtrC sample concentration indicated. Scans were recorded every 4 h and equilibrium was considered to have been reached when the absorbance values remained constant over a 4-h period. After equilibrium had been reached, five scans were recorded for each sample. The program ULTRASCAN 6.2 [31] was used to simultaneously fit the sedimentation equilibrium profiles obtained at three different speeds, to a single-species, non-interacting system. The molecular weight was determined by fitting the absorbance data of the equilibration runs using the exponential equation

$$C(r) = C(r_0) \cdot e^{\left(\frac{(1-\nu\rho)\omega^2}{2RT}M(r^2-r_0^2)\right)}, \quad (1)$$

where $C(r)$ is the concentration at radius r , $C(r_0)$ is the concentration at reference radius r_0 , M is the monomer molecular weight, R is the universal gas constant, T is the temperature, ω is the angular velocity, ρ is the density of the solution and ν is the partial specific volume of the protein. Rearranging this equation gives

$$\frac{d \ln(Cr)}{dr^2} = \frac{M(1-\nu\rho)\omega^2}{2RT}. \quad (2)$$

For visualizing the data graphically, measured absorbance can be substituted for concentration and plots of log absorbance versus $r^2 - r_0^2/2$ for a single species are expected to give a straight line, the slope of which is proportional to the molecular mass of the protein.

Protein film voltammetry

Protein film voltammetry (PFV) was performed as described previously [32] except that the working electrode surface (geometric area 0.12 cm^2) was freshly polished basal-plane graphite. Protein films were prepared using a Hamilton syringe to apply an approximately 1 μL aliquot of an ice-cold 40 μM MtrC solution in 50 mM HEPES, 100 mM NaCl, 0.5% (wt/vol) CHAPS, pH 7.0 to the electrode surface. Buffer–electrolyte solutions were brought to the desired pH by the addition of aliquots of 2 M NaOH or 2 M HCl. The influence of pH was investigated in solutions composed of 50 mM 2-morpholinoethanesulfonic acid (MES) (pH 6.0), HEPES (pH 7.0 and pH 8.0), *N*-cyclohexyl-2-aminoethanesulfonic acid (CHES) (pH 9.0) or 3-(cyclohexyl)-1-aminopropanesulfonic acid (CAPS) (pH

10.0 and pH 11.0), all with 100 mM NaCl as electrolyte. The pH was monitored prior to and following voltammetric experiments and remained constant. Voltammetric responses were unchanged when the buffer–electrolyte was switched from 100 mM NaCl to 350 mM NaCl. Stock solutions of iron(III) citrate were prepared by dissolving iron(III) chloride 6-hydrate (98% purity, Sigma) and citric acid (99.7% purity, Sigma) in deionized water to give a stock solution of 1:1 molar ratio. The pH of the resulting solution was brought to 7.0 by additions of a 10 M NaOH solution. Following preparation, solutions were filtered through a 0.22- μm nylon syringe filter and stored in light-free conditions. Faradaic voltammetric responses were extracted from raw data using the The Utilities for Data Analysis 010716 program, kindly provided by H.A. Heering. Engineered “reticulating (cubic splines)” baselines, retaining the experimental baseline character, were constructed and subtraction from experimental voltammograms yielded the Faradaic response of MtrC.

Results

Purification and biochemical characterization of MtrC

Membrane fractions of *S. oneidensis* MR-1 were solubilized in CHAPS detergent and initially purified on a (diethylamino)ethyl anionic exchange column. Eluted fractions containing MtrC were purified further on Q-Sepharose and S200 columns. The purified protein obtained migrated in SDS-PAGE gels as an approximately 75 kDa Coomassie blue staining band (Fig. 2a, inset, lane 2) that also stained for heme-dependent peroxidase activity (Fig. 2a, inset, lane 3). The polypeptide was positively identified as MtrC by peptide fragmentation mass analysis (not shown) and via detection with MtrC-specific antibodies (Fig. 2a, inset, lane 4). The final yields of purified MtrC were routinely 5–10 mg L⁻¹ starting culture. MtrC preparations could be stored at 193 K for prolonged periods (more than 6 months) without noticeable deterioration, as judged by UV–vis absorption spectroscopic properties and SDS-PAGE. Highly concentrated samples could be prepared (more than 0.5 mM) without evidence of precipitation, indicating the suitability of the 20 mM HEPES, 100 mM NaCl, 0.5% (wt/vol) CHAPS, pH 7.5 buffer–electrolyte–detergent system used.

The air-oxidized MtrC UV–vis spectrum displays a heme Soret (γ) absorption peak centered at 410 nm, a visible-region peak at 531 nm and a shoulder at 560 nm (Fig. 2a). This spectrum remains unaltered upon further oxidation of MtrC by potassium ferricyanide (data not shown). When MtrC is reduced with dithionite, the Soret (γ) peak shifts to 419 nm and clearly defined α and β peaks

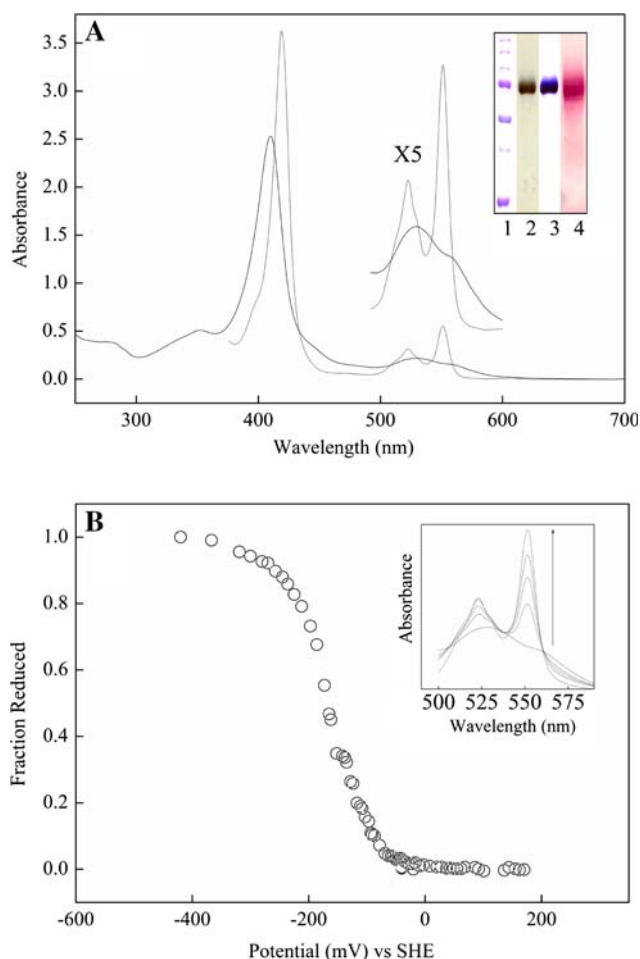


Fig. 2 UV–vis properties of MtrC. **a** UV–vis absorption spectrum of MtrC (2 μM) in 50 mM HEPES, pH 7.5, 100 mM NaCl, 0.5% (wt/vol) CHAPS. Solid line air-oxidized MtrC, dashed line sodium dithionite reduced MtrC. Also shown is $\times 5$ amplification of the 500–600-nm absorption region. Inset: lanes 1–3 sodium dodecyl sulfate polyacrylamide gel electrophoresis (SDS-PAGE) analysis of purified *Shewanella oneidensis* MR-1 MtrC. Lane 1 molecular mass markers (from top to bottom: 250, 150, 100, 75, 50, 37 and 25 kDa); lane 2 heme-stained purified MtrC; lane 3 Coomassie blue stained purified MtrC; lane 4 purified MtrC resolved by SDS-PAGE, electroblotted and detected with anti-MtrC primary and goat-anti rabbit alkaline phosphatase secondary antibodies. **b** UV–vis spectropotentiometric properties of MtrC. Fraction of MtrC reduced versus potential (vs. the standard hydrogen electrode, SHE). Inset UV–vis absorption spectrum of MtrC focusing on the 500–600-nm region obtained at +241, -110, -140, -160 and -210 mV. The direction of the arrow indicates spectra collected at an increasingly negative potential. Conditions of measurement were as follows: MtrC (2 μM) in 100 mM HEPES, pH 7.5, 100 mM NaCl, 0.5% (wt/vol) CHAPS

are observed at 552 and 523 nm (Fig. 2a). The absorbance ratio of heme to total protein (410 nm/280 nm) of oxidized protein was typically approximately 7.0 and an extinction coefficient at 410 nm of 1,260 mM⁻¹ cm⁻¹ was experimentally determined. The pyridine hemochrome of MtrC displays an α absorption peak at 550 nm typical of low-

spin *c*-type cytochromes [26, 27]. Quantitative analysis suggests the covalent attachment of 10.8 (average value from five repeat experiments) *c* hemes correlating with the ten predicted CXXCH heme attachment sequences encoded within the protein sequence.

The continuous-wave, 2 mW, 10 K perpendicular mode X-band EPR spectrum was dominated by a broadened rhombic-type signal with *g* values tentatively ascribed as follows: $g_1 \sim 3.2, 3.0$ and 2.86 ; $g_2 \sim 2.20$; and $g_3 \sim 1.5$ (Fig. 3a). The broadness and asymmetry of the $g_{\max} \sim 3.7$ – 2.7 region is consistent with a composite signal arising from multiple resonances of low-spin *c*-heme paramagnetic species [33]. The defining features of this spectrum were unchanged in ferricyanide-oxidized samples and were concentration-independent (except for signal: noise) over the range 20–100 μM . At increased microwave power (32 mW) the broadness of the $g_{\max} \sim 3.7$ – 2.7 region was reduced slightly, with the signal intensity of $g \sim 3.2$ and 2.86 features decreasing relative to that of the $g \sim 3.0$ feature. Signals due to small amounts of high-spin Fe(III) heme and adventitious Fe(III) are observed at $g \sim 6$ and $g \sim 4.3$.

The relative sensitivities of UV–vis absorption and EPR spectroscopy required an increased sample concentration for EPR analysis (more than 20 μM compared with less than 5 μM for UV–vis absorption spectroscopy). To assess the MtrC oligomeric conformation over this concentration range, analytical ultracentrifugation (sedimentation equilibrium) analysis was employed. Sedimentation equilibrium profiles of MtrC samples were collected at three rotor speeds (6,000, 8,000 and 10,000 rpm) for five different MtrC concentrations (3, 10, 20, 40 and 60 μM). For each MtrC concentration, the sedimentation data collected at the three rotor speeds were simultaneously fitted to a single-species, noninteracting model. Plots of log absorbance versus $r^2 - r^2(\text{ref})/2$ (Fig. 4) are expected to give a straight line, the slope of which is proportional to the molecular mass of the protein [34]. Straight-line plots with similar gradients were obtained for all five MtrC concentrations examined (Fig. 4) with the best fits yielding molecular masses of 96, 90, 89, 89 and 89 kDa for the 3, 10, 20, 40 and 60 μM samples, respectively. These observed molecular masses are close to that predicted for the MtrC polypeptide with ten hemes covalently attached (approximately 85 kDa) and suggest a monomeric state within the concentration range examined. The 5–10 kDa of additional observed mass may be attributed to MtrC-associated CHAPS detergent.

Thermodynamic properties of MtrC

A potentiometric titration, monitored by UV–vis absorption spectroscopy, was performed to assess the thermodynamic

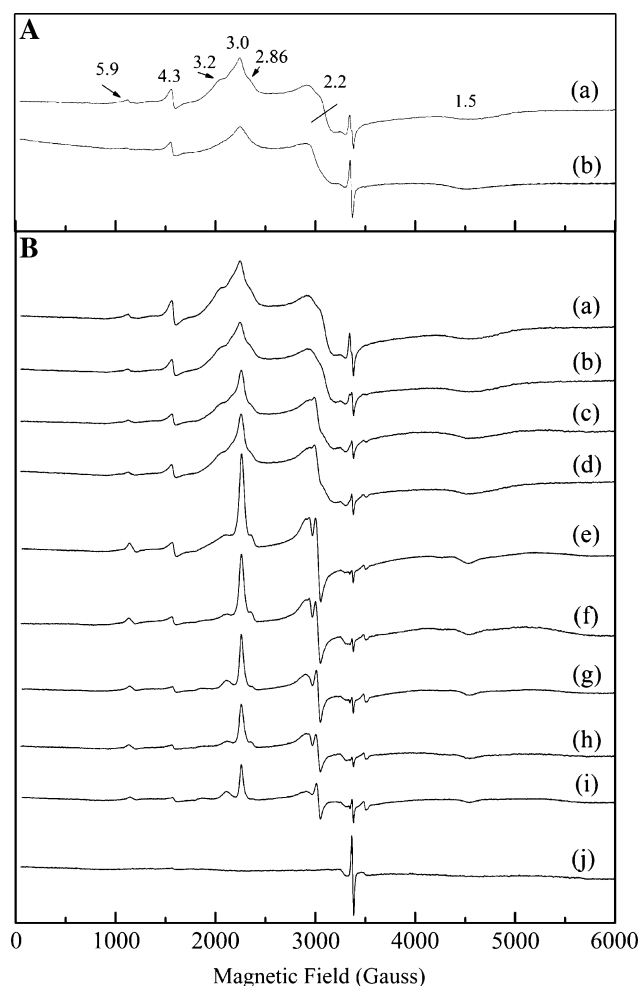


Fig. 3 Continuous-wave X-band electron paramagnetic resonance (EPR) properties of MtrC. **a** X-band EPR signals arising from purified MtrC. **a** MtrC spectrum collected at +200 mV. Conditions of measurement as follows: MtrC (140 μM) in 50 mM HEPES, pH 7.5, 100 mM NaCl, 0.5% (wt/vol) CHAPS, temperature 10 K, microwave power 2 mW, microwave frequency 9.68 GHz and modulation amplitude 10 G. **b** Sample and conditions of measurement as for **a** above but the spectrum was collected at 32-mW microwave power. **b** EPR spectra of MtrC poised at **a** +100 mV, **b** 0 mV, **c** –100 mV, **d** –150 mV, **e** –175 mV, **f** –200 mV, **g** –300 mV, **h** –400 mV, **i** –450 mV and **j** –500 mV. The sharp derivative at $g \sim 2$ in **j** arises from reduced mediators. Conditions of measurement as follows: MtrC (140 μM) in 50 mM HEPES, pH 7.5, 100 mM NaCl, 0.5% (wt/vol) CHAPS, temperature 10 K, microwave power 2 mW, microwave frequency 9.68 GHz and modulation amplitude 10 G

properties of MtrC in solution. UV–vis absorption spectra of MtrC were obtained at a range of potentials spanning between +400 and –450 mV and the normalized α -peak absorbance was plotted versus potential (Fig. 2b). Spectra at all potentials studied were typical of low-spin *c*-type hemes and the maximum α -peak absorbance wavelength and shape did not change during the titration (Fig. 2b, inset). The MtrC hemes are reduced over a potential

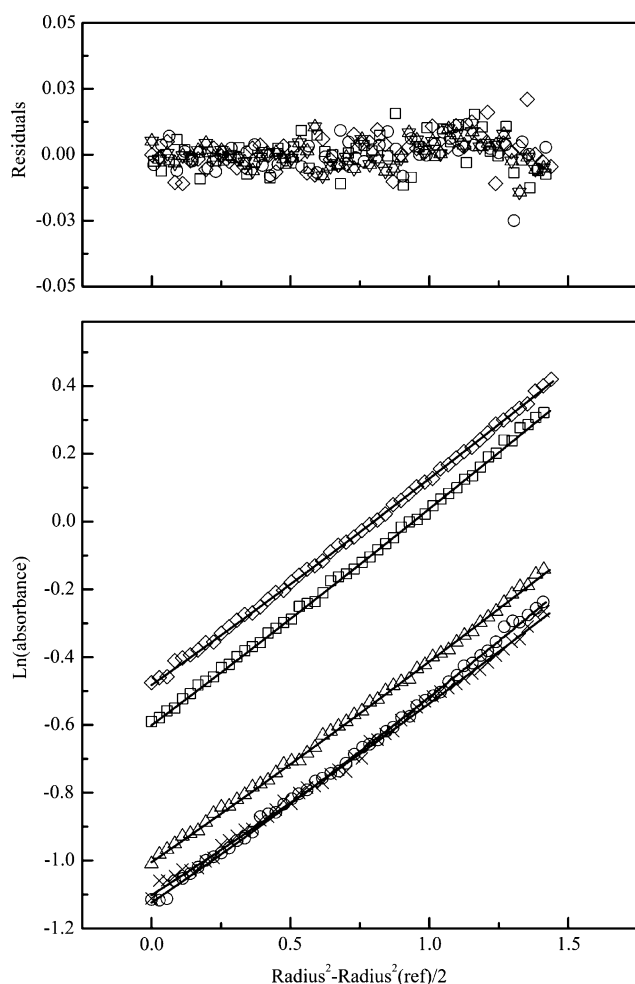


Fig. 4 Analytical ultracentrifugation (sedimentation equilibrium) analysis of MtrC. *Lower panel:* Absorbance profiles of MtrC at concentrations of 3 μM (circles), 10 μM (squares), 20 μM (diamonds), 40 μM (triangles) and 60 μM (crosses) measured at 440, 530, 495, 600 and 620 nm, respectively. For each concentration the data were globally fitted from centrifugation runs at 6,000, 8,000 and 10,000 rpm (16 h at 293 K) to the equation for a single-species, non-interacting model (solid lines). Conditions of measurement as follows: MtrC samples in 50 mM HEPES, pH 7.5, 150 mM NaCl, 0.5% (wt/vol) CHAPS. *Upper panel:* Residuals between the experimental data and the fitted lines

window spanning approximately 500 mV, from fully oxidized (+100 mV) to fully reduced (−400 mV) (Fig. 2b). A simple monoheme protein ($n = 1$) titrates over approximately 200 mV [27]. The broad potential range covered by MtrC redox chemistry reflects the presence of multiple heme centers with overlapping redox potentials, such that the contribution of individual hemes cannot be resolved. Multiple sequence alignments of MtrC homologues reveal the presence of 20 conserved histidines, ten in the CXXCH motifs and ten elsewhere in the primary structure. This would satisfy the required ligand sets for ten bishistidine-ligated low-spin c -type hemes. The electron-donating properties of histidine imidazole-ring nitrogen ligands to

the heme iron stabilizes the oxidized Fe(III) state over the reduced Fe(II) state, thus resulting in more negative heme redox potentials compared with those of histidine–methionine-coordinated hemes [27]. Bishistidine heme coordination is thus consistent with the observed MtrC heme redox potentials.

Protein film voltammetry was also used to probe the redox chemistry of MtrC. Cyclic voltammograms of MtrC adsorbed onto a basal-plane graphite electrode and following subtraction of capacitive current revealed clear peaks corresponding to reduction (cathodic current) and oxidation (anodic current) of adsorbed MtrC molecules (Fig. 5, panel A). Signals were unchanged by electrode rotation or transfer of the MtrC-coated electrode to fresh buffer–electrolyte solution and were not observed in the absence of MtrC, which allows the signals to be attributed to direct redox transformation of MtrC. Exploration of more positive and negative potentials failed to identify additional redox activity from MtrC. The peak areas are almost identical for oxidative and reductive sweeps and hence the Faradaic current results from the stoichiometric reduction and oxidation of the MtrC hemes. Irrespective of pH, a typical reduction or oxidation wave integrates to approximately $2 \mu\text{C cm}^{-2}$, from which MtrC coverage of the electrode is calculated as approximately 2 pmol cm^{-2} . This is consistent with the formation of an electroactive monolayer of a protein the size of MtrC (approximately 85 kDa).

At pH 7.0, PFV shows that the complete reduction and subsequent reoxidation of MtrC hemes occurs between approximately +200 and −400 mV (vs. SHE). Again this is a much broader potential window (approximately 600 mV) than that anticipated for an independently titrating single-electron center (approximately 200 mV) [35, 36]. As in the UV–vis absorption monitored potentiometric titration (Fig. 2b), this is consistent with the hemes within MtrC displaying a range of overlapping reduction potentials that contribute to the signal in an unresolved manner. Transfer of MtrC-coated electrodes into buffer–electrolyte of increasingly alkaline pH resulted in a negative shift of the noncatalytic signals, while the overall peak areas are retained (Fig. 5, panel B). The peaks display defined shoulders at pH 10 and 11, illustrating that the heme redox potentials span a wider range here than at pH 7. Coupling the transfer of one electron to one proton results in a uniform shift in peak potential of approximately −48 mV per pH unit [35, 36]. The observation that the heme reduction potentials are more disparate at alkaline pH suggests the reduction of certain hemes within MtrC is coupled to protein protonation.

UV–vis monitored spectropotentiometry and noncatalytic PFV analyses provide information on the potential window over which MtrC is redox-active under conditions

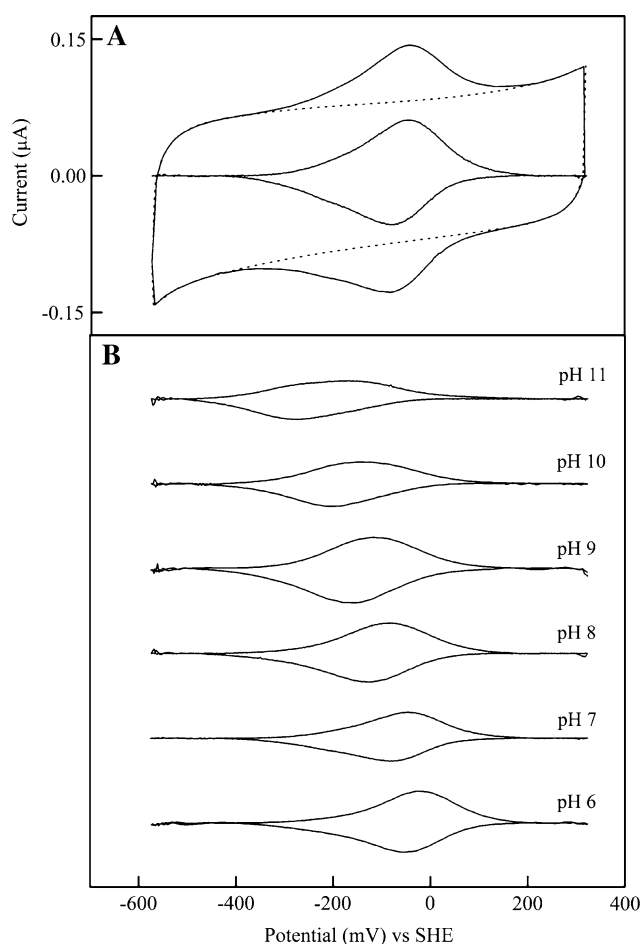


Fig. 5 Noncatalytic protein film voltammetry of MtrC. **A** Cyclic voltammogram of adsorbed MtrC. The *dotted line* is the electrode response in the absence of an MtrC protein film. The buffer-electrolyte is 50 mM HEPES, 100 mM NaCl, pH 7.0; scan rate 30 mV s^{-1} , temperature 273 K. In the *middle* is the bare electrode “baseline” response subtracted from the MtrC coated electrode response. **B** The effect of pH on MtrC cyclic voltammetry. Representative baseline-subtracted, normalized responses of MtrC in 100 mM NaCl, 50 mM MES, HEPES, CHES or CAPS at pH 6.0, 7.0, 8.0, 9.0, 10.0 and 11.0 as indicated; scan rate 30 mV s^{-1} , temperature 273 K

in which potential control over the sample is imposed while the analysis is performed. However, neither technique resolves the behavior of individual (sets of) hemes. For this reason samples of MtrC were poised electrochemically at defined potentials in a carbon pot and transferred to EPR tubes for spectroscopic analyses (Fig. 3b). As the potential of the poised sample was lowered from +100 to -150 mV , the broad $g_{\text{max}} \sim 3.7\text{--}2.7$ region changed shape, most notably decreasing in breadth. For samples poised at potentials of -150 and -175 mV the shape change becomes more dramatic, with a sharp, intense resonance appearing at $g = 2.9$ and an associated derivative signal appearing at $g = 2.2$ (Fig. 3b, spectra d, e). These EPR signals are characteristic of the g_1 and g_2 components of

rhombic signals arising from low-spin bishistidine-ligated Fe(III) hemes with near-parallel imidazole planes [27, 33]. The appearance of these features during the reductive titration is suggestive of magnetic coupling between two, or more, low-spin heme centers in the fully oxidized protein [37]. For example, if two magnetically spin-coupled low-spin Fe(III) hemes have sufficiently distinct reduction potentials, reduction of one of these hemes to the $S = 0$ low-spin Fe(II) state “uncouples” the previously EPR-silent spin-coupled $S = 1/2$ Fe(III) heme.

In MtrC samples poised below -175 mV the intensity of the $g = 2.9$ and 2.2 resonances decreased progressively (Fig. 3b, spectra e–j). Owing to the overlap with other signals, accurate integration of the rhombic trio at $g = 2.9$, 2.2 and 1.5 was prevented for samples poised above -400 mV . However, the signal was sufficiently resolved in the sample poised at -450 mV to allow informative integration and this yielded a value of 1.3 hemes per MtrC molecule. Given that the signal intensity of the sample poised at -450 mV accounts for approximately 40% of the signal intensity from the sample poised at -175 mV (Fig. 3b, spectrum e), we tentatively attribute contributions from up to three magnetically isolated $S = 1/2$ Fe(III) hemes to the signal seen at the higher potential. While the EPR spectra from MtrC are clearly complex, with more features than we have discussed explicitly here, we have succeeded in resolving contributions from spin-coupled and magnetically isolated hemes over distinct potential ranges. Many of the EPR-detectable hemes titrate over a similar potential range to that evident from the UV-vis/PFV analyses. Exceptions are those hemes that are still EPR-detectable, i.e., oxidized, in samples poised below -400 mV . However, in these experiments potential control is lost as soon as the sample is removed from the carbon pot for transfer to the EPR tube. Thus, it is quite possible that some positive drift of the sample potential occurs prior to EPR analysis and that this is likely to be more pronounced in samples poised at the lower, as opposed to higher, potentials. With this in mind, the results of both spectropotentiometric analyses and PFV appear to be in good agreement.

Electron transfer kinetics of MtrC

To examine the ability of MtrC to transfer electrons to a solid electrode surface, interfacial electron transfer kinetics were probed using PFV. By monitoring the position of the reductive (E_p^c) and oxidative (E_p^a) peaks as a function of scan rate (Fig. 6) and using Trumpet plot analysis [38], we estimate a standard heterogeneous rate constant of approximately 100 s^{-1} . The overlapping contribution from ten heme centers under each peak prevents rigorous kinetic quantitation; however, the value is within the range

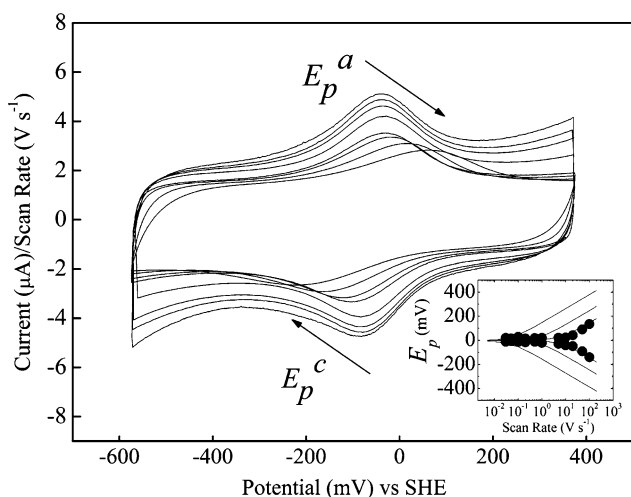


Fig. 6 The scan-rate dependence of MtrC noncatalytic protein film voltammetry. Cyclic voltammograms of MtrC at scan rates of 0.03, 0.05, 0.1, 0.5, 10, 20, 50 and 100 V s^{-1} . The arrows indicate increasing scan rate. Inset: Variation of the oxidative (E_p^a) and reductive (E_p^c) peak potentials with scan rate. Trumpet plots were generated with heterogeneous rate constants of 1 s^{-1} , 10 s^{-1} and 100 s^{-1} . Buffer–electrolyte 50 mM HEPES, 100 mM NaCl, pH 7.0, 273 K

displayed by intracellular redox proteins considered to undergo facile interfacial electron exchange in similar experiments [36] and indicates that MtrC contains a heme arrangement compatible with facile electron exchange with solid surfaces.

Electron transfer kinetics were probed further in voltammetric experiments in which the electrode substituted the role of intracellular electron transfer proteins in delivering electrons to MtrC. The subsequent rate at which MtrC could mediate electron transfer to iron(III) citrate, a model respiratory Fe(III) substrate of *S. oneidensis* MR-1 [11, 17], was then quantitated. Iron(III) citrate speciation is complex, with a number of different mononuclear and polynuclear species able to form in aqueous solution in a concentration-dependent manner [39]. Nevertheless, well-defined “sigmoidal” reduction waves were observed when MtrC-coated electrodes were placed in solutions of iron(III) citrate and rotated at 3,000 rpm (to negate substrate mass-transport effects) (Fig. 7). Significantly, the steepest region of the catalytic wave corresponds to the potential window where the nonturnover peaks from MtrC are observed, indicating that in the presence of substrate, as hemes are reduced, the enzyme is “switched on” (Fig. 7a). Voltammetry of iron(III) citrate solutions with rotated “bare” graphite electrodes in the absence of MtrC films displayed iron(III) citrate reduction, but this nonspecific response was always clearly distinguishable in shape from that of the MtrC-mediated catalytic response (Fig. 7a). Analysis of the magnitude of the catalytic current was

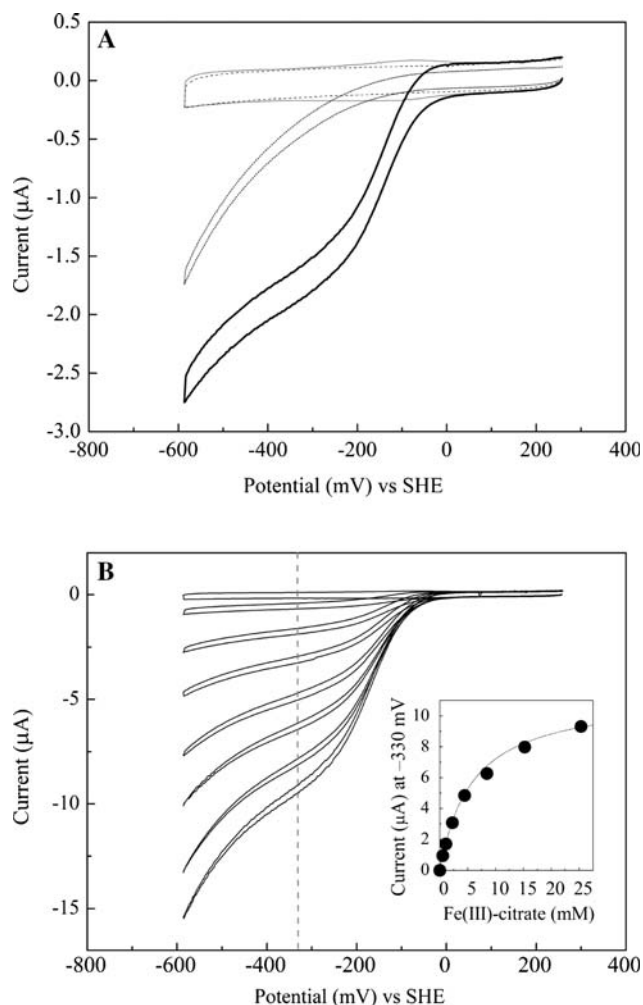


Fig. 7 Catalytic protein film voltammetry of MtrC. **a** Typical cyclic voltammograms illustrating the reduction of 1 mM iron(III) citrate by MtrC adsorbed on a basal-plane graphite electrode (*heavy solid line*) and by the basal-plane graphite electrode in the absence of adsorbed MtrC (*dotted line*). Also displayed are the voltammetric responses of MtrC in the absence of iron(III) citrate (*light solid line*) and the bare electrode in the absence of MtrC and iron(III) citrate (*dashed line*). **b** Typical cyclic voltammograms from an MtrC film in 0, 0.5, 1, 2, 4.5, 9, 16 and 25 mM iron(III) citrate. The electrochemical potential (-330 mV) where the catalytic current was analyzed is illustrated by a *broken gray line*. Inset: Variation of the magnitude of the catalytic current, measured at -330 mV , with iron(III) citrate concentration. The line describes the catalytic current arising from a Michaelis–Menten description of enzyme kinetics with a Michaelis constant of 6 mM and a turnover number of 430 s^{-1}

performed at -330 mV to minimize reductive contributions to the current from the bare electrode while maximizing the contribution from MtrC. The current at -330 mV in the presence of MtrC, but prior to iron(III) citrate addition, was taken as the zero-substrate response. The catalytic current (rate) displayed saturating behavior on increasing the iron(III) citrate concentration (Fig. 7b).

Fitting to the Michaelis–Menten equation yielded a Michaelis constant of 6 ± 2 mM and a turnover number of 430 s^{-1} . These numbers should be considered as upper limits for these kinetic parameters since we cannot exclude some contribution to catalytic currents from electrodic reduction of iron(III) citrate at the higher concentrations used.

It is clear that MtrC can achieve a rate of iron(III) citrate reduction comparable to that achieved by intracellular respiratory reductases with their substrates. No MtrC-dependent catalytic currents could be observed with nitrate or nitrite, alternative respiratory substrates of *S. oneidensis*. Efforts to explore “solid” Fe(III) substrates, such as amorphous iron(III) oxide, were hindered by interference from electrodic reduction. Nevertheless, the results demonstrate that MtrC can mediate electron transfer to an Fe(III) substrate in a potential window that corresponds with the redox properties of the enzyme determined from equilibrium potentiometric titrations. The results are consistent with the reduced capacity of *S. oneidensis* to grow on iron(III) citrate in $\Delta mtrC$ mutants [11, 17].

Discussion

The spectropotentiometric and voltammetric analysis of MtrC provides the first insights into the thermodynamic and kinetic properties of the multiheme cytochrome proposed to mediate electron transfer to extracellular electron acceptors. Solution-state potentiometry and PFV revealed that the hemes within MtrC reversibly titrate between fully oxidized and fully reduced states over a redox potential range of approximately +100 and -400 mV (vs. SHE). This broad potential range reflects the composite titrations of ten hemes that precludes resolution of individual heme redox potentials. It could be argued that the operating potentials of the MtrC hemes would be significantly modified on engagement with a solid mineral surface. Our view is that any change will be negligible since we find MtrC redox activity occurs over a similar potential range when MtrC is in solution, monitored using UV–vis spectropotentiometry, and when it is adsorbed on a solid surface, probed using PFV. It is interesting to note that whole-cell voltammetry of *Shewanella* species anaerobically grown (conditions where we would expect MtrC to be synthesized) and adsorbed on glassy carbon electrodes revealed reversible reduction and oxidation peaks centered at approximately -100 mV (vs. SHE) [24, 25], a similar behavior to that presented here for MtrC. This suggests that intact cells with MtrC exposed on the outer-cell surface exchange electrons with solid substrates over a similar potential window as the redox chemistry determined here for the purified protein.

EPR spectropotentiometry of MtrC gave complex spectra that included signals likely to arise from magnetically isolated and magnetically interacting hemes. Complex heme–heme interactions have been reported in other multiheme cytochromes such as the decaheme NrfA homodimer [40] and the 24-heme hydroxylamine oxidoreductase homotrimer [37, 41] and it is only through structure-based spectral deconvolutions that spectral features have been assigned to individual heme pairs or triads [40, 41]. At present, despite extensive efforts, the structure of MtrC is not known; however, primary structure analysis suggests that it, and also periplasmic decaheme MtrA [10], encodes two approximately 150 amino acid pentaheme modules with similarity to the pentaheme NrfB, an approximately 150 amino acid pentaheme periplasmic electron transport cytochrome widely involved in nitrite respiratory systems. All five hemes within NrfB are bishistidine-coordinated and it exhibits thermodynamic activity over a similar potential domain to MtrC [42].

Like MtrC, the other multiheme cytochromes suggested to be involved in transferring electrons to the outer membrane from MQH₂ in the inner membrane also bind bishistidine-coordinated low-potential hemes. These proteins include CymA, a tetraheme *c*-type cytochrome anchored to the inner membrane that serves as a MQH₂ dehydrogenase [8, 12, 20, 43, 44]; Stc, a 12-kDa tetraheme periplasmic *c*-type cytochrome [15, 45] and the periplasmic decaheme cytochrome MtrA [10] (Fig. 1). CymA is not thought to be a proton-motive quinol dehydrogenase and thus the electron transfer from quinol to MtrC is not energy conserving. Depending on growth conditions, electrons could enter the MQH₂ pool via the activity of primary dehydrogenases, such as NADH dehydrogenase, formate dehydrogenase or hydrogenase. The redox potential of the NAD⁺/NADH, CO₂/HCOO⁻ or 2H⁺/H₂ couples in the cell will be approximately -300 to -400 mV and that of MQ/MQH₂ approximately -50 to -100 mV. This thermodynamic free energy gap ($\Delta E \sim 300$ – 400 mV) is sufficient to allow for generation of a proton-motive force (approximately 200 mV) through coupling electron transport to either proton translocation (NADH dehydrogenase) or an electrogenic redox loop (formate dehydrogenase or hydrogenase) (Fig. 1). Thus, in terms of bioenergetics, the energy-conservation associated with respiration of extracellular Fe(III) is most likely to be associated with electron input into the MQ pool (reduction of MQ to MQH₂), with the multiheme conduit linking MQH₂ to Fe(III) minerals simply serving to harness Fe(III) reduction as a means to recycle MQ (Fig. 1). This makes it bioenergetically equivalent to the well-characterized bacterial periplasmic nitrate reductase system [5] that is also present in *S. oneidensis* MR-1 (Fig. 1). At this stage the actual operating potentials of individual hemes in the conduit is unknown,

since injection of one electron into a multiheme cytochrome can change the potential of a neighboring heme. This has been studied in some detail for hydroxylamine oxidoreductase and the tetraheme cytochrome *c*-554 [46] and could be yet more complex for a decaheme cytochrome. Furthermore, it is not clear if all the hemes in the system need be involved. Nevertheless the role for Fe(III) reduction in recycling the MQ pool negates the need for a large ΔE between the MQH₂ and the multiheme cytochrome chain to drive a proton-motive step. There simply needs to be sufficient driving force to allow electron transfer to proceed through the low-potential heme conduit and this can be envisaged when the MQ/MQH₂ is predominantly reduced and there is strong oxidant such as an Fe(III) mineral oxide to draw electrons through the system.

In closing, it is not immediately clear why MtrC need be a decaheme cytochrome to achieve the one-electron reduction of Fe(III). In the intact cell, MtrC will receive electrons from the CymA-Stc-MtrA conduit that mediates electron transfer between the inner and the outer membrane and the multiheme nature of this conduit may represent an efficient means to achieve electron transfer across the approximately 150 Å that separates these two membranes (Fig. 1). It may be that the multiheme nature of the outer-membrane MtrC is also important for moving electrons long distances, but in this case this might be away from the outer membrane through extracellular lipopolysaccharide to the extracellular substrate. Having an extracellular enzyme with many hemes available as potential one-electron output sites may also serve to facilitate productive interaction with minerals in the environment that are likely to present chemically and topographically diverse substrates. Further insights into the role of the ten hemes will require the resolution of the tertiary structure to MtrC to resolve the molecular organization of these cofactors.

Acknowledgements This work was supported by Schlumberger, the US Department of Energy Biogeochemistry Grand Challenge, the UK Biotechnology and Biological Sciences Research Council grants B18695 and BBSSA200410938 and a JIF award (062178). The Pacific Northwest National Laboratory is operated for the Department of Energy by the Battelle Memorial Institute, contract DE-AC05-76RLO1830. We thank Ann Reilly for invaluable technical support and Andy Gates and Clive Butler for valuable help and discussion.

References

- Venkateswaren K, Moser DP, Dollhopf ME, Lies DP, Saffarini DA, Macgregor BJ, Ringelberg DB, White DC, Nishijima M, Sano H et al (1999) *Int J Syst Bacteriol* 49:705–724
- Nealson KH, Scott J (2003) In: Dworkin M (ed) *The prokaryotes*, vol 2004. Springer, New York
- Heidelberg JF, Paulsen IT, Nelson KE, Gaidos EJ, Nelson WC, Read TD, Eisen JA, Seshadri R, Ward N, Methe B, Clayton RA et al (2002) *Nat Biotechnol* 20:1118–1123
- Nealson KH, Belz A, McKee B (2002) *Antonie Van Leeuwenhoek Int J Gem M* 81:215–222
- Richardson DJ (2000) *Microbiol* 146:551–571
- Nealson KH, Saffarini D (1994) *Annu Rev Microbiol* 48:311–343
- Fredrickson JK, Zachara JM, Kennedy DW, Dong HL, Onstott TC, Hinman NW, Li SM (1998) *Geochim Cosmochim Acta* 62:3239–3257
- Myers C, Myers J (1992) *J Bacteriol* 174:3429–3438
- Myers C, Myers J (1993) *FEMS Microbiol Lett* 108:15–22
- Pitts KE, Dobbin PS, Reyes-Ramirez F, Thomson AJ, Richardson DJ, Seward HE (2003) *J Biol Chem* 278:27758–27765
- Beliaev AS, Saffarini DA, McLaughlin JL, Hunnicutt D (2001) *Mol Microbiol* 39:722–730
- Myers CR, Myers JM, (1997) *J Bacteriol* 179:1143–1152
- Myers CR, Myers JM (2003) *Lett Appl Microbiol* 37:254–258
- Gordon EHJ, Pike AD, Hill AE, Cuthbertson PM, Chapman SK, Reid GA (2000) *Biochem J* 349:153–158
- Tsapin AI, Vandenberghe I, Nealson KH, Scott JH, Meyer TE, Cusanovich MA, Harada E, Kaizu T, Akutsu H, Leys D, Van Beeumen JJ (2001) *Appl Environ Microbiol* 67:3236–3244
- Dobbin PS, Butt JN, Powell A, Reid GA, Richardson DJ (1999) *Biochem J* 342:439–448
- Myers JM, Myers CR (2002) *Appl Environ Microbiol* 68:2781–2793
- Myers JM, Myers CR (2001) *Appl Environ Microbiol* 67:260–269
- Beliaev AS, Saffarini DA (1998) *J Bacteriol* 180:6292–6297
- Field SJ, Dobbin PS, Cheesman MR, Watmough NJ, Thomson AJ, Richardson DJ (2000) *J Biol Chem* 275:8515–22
- Shi L, Chen B, Wang Z, Elias DA, Mayer MU, Gorby YA, Ni S, Lower BH, Kennedy DW, Wunschel DS, Mottaz HM, Marshall MJ, Hill EA, Beliaev AS, Zachara JM, Fredrickson JK, Squier TC (2006) *J Bacteriol* 188:4705–4714
- Myers CR, Myers JM (2004) *Lett Appl Microbiol* 39:466–70
- Kim HJ, Park HS, Hyun MS, Chang IS (2002) *Enzyme Microb Technol* 30:145–152
- Kim BH, Kim HJ, Hyun MS, Park DH (1999) *Microbiol Biotechnol* 9:127–131
- Shi L, Lin JT, Markillie LM, Squier TC, Hooker BS (2005) *Biotechniques* 38:297
- Berry E, Trumpower B (1987) *Anal Biochem* 161:1–15
- Moore GR, Pettigrew GW (1990) *Cytochromes c: evolutionary, structural and physicochemical aspects*. Springer, New York
- Dutton PL (1978) *Methods Enzymol* 54:411–435
- Aasa R, Vanguard T (1975) *J Magn Reson* 19:308–315
- Philo JM (1997) *Biophys J* 72:435–444
- Demeller B (2005) <http://www.ultrascan.uthscsa.edu/>
- Anderson LJ, Richardson DJ, Butt JN (2001) *Biochemistry* 40:11294–11307
- Walker FA (1999) *Coord Chem Rev* 186:471–534
- Horan T, Wen J, Arakawa T, Liui N, Brankow D, Hu S, Ratzkin B, Philo JS (1995) *J Biol Chem* 270:24604–24608
- Almeida MG, Silveira CM, Guigliarelli B, Bertrand P, Moura JIG, Moura I, Leger C (2007) *FEBS Lett* 581:284–288
- Bard AJ, Faulkner LR (2001) *Electrochemical methods: fundamentals and applications*, 2nd edn. Wiley, New York
- Hendrich MP, Petasis D, Arciero DM, Hooper AB (2001) *J Am Chem Soc* 123:2997–3005
- Hirst J, Armstrong FA (1998) *Anal Chem* 70:5062–5071
- Gautier-Luneau I, Merle C, Phanon D, Lebrun C, Biaso F, Sertratrice G, Pierre JL (2005) *Chemistry* 11:2207–2219
- Bamford VA, Angrove HC, Seward HE, Thomson AJ, Cole JA, Butt JN, Hemmings AM, Richardson DJ (2002) *Biochemistry* 41:2921–2931
- Hendrich MP, Logan M, Andersson KK, Arciero DM, Lipscomb JD, Hooper AB (1994) *J Am Chem Soc* 116:11961–11968

42. Clarke TA, Dennison V, Seward HE, Burlat B, Cole JA, Hemmings AM, Richardson DJ (2004) *J Biol Chem* 279:41333–41339
43. Myers CR, Myers JM (1994) *J Appl Bacteriol* 76:253–258
44. Schwalb C, Chapman SK, Reid GA (2003) *Biochemistry* 42:9491–9497
45. Leys D, Meyer TE, Tsapin AS, Neelson KH, Cusanovich MA, Van Beeumen JJ (2002) *J Biol Chem* 277:35703–25711
46. Kurnikov IV, Ratner MA, Pacheco A (2005) *Biochemistry* 44:1856–1863